Comput Mech
DOI 10.1007/s00466-008-0282-2

ORIGINAL PAPER

Numerical modelling of acoustic–elastodynamic coupled problems by stabilized boundary element techniques

D. Soares Jr

Received: 22 May 2007 / Accepted: 14 March 2008

Abstract In this work, an efficient, flexible, accurate and stable algorithm to numerically model interacting acoustic–elastodynamic sub-domains is described. Stabilized time-domain boundary element techniques are considered to discretize each sub-domain of the model and proper numerical expressions on acoustic–elastodynamic interfaces are presented. Moreover, stabilized iterative coupling procedures are adopted and different time and space sub-domain discretizations are allowed, improving the robustness and versatility of the methodology. At the end of the paper, numerical results are presented, illustrating the potentialities of the proposed formulation.

Keywords Time-domain BEM · Iterative BEM–BEM coupling · Acoustics · Elastodynamics · Stabilized formulations · Fluid–solid interaction

1 Introduction

Time-domain numerical modelling of wave propagation in highly heterogeneous media requires robust simulation algorithms in order to preserve accuracy, efficiency and stability.

In a Finite Difference Method (FDM) context, Lombard and Piraux [1] list the following main reasons for low confidence results in a situation where there is discontinuity of physical properties: spurious diffractions occur due to the stair-step representation of arbitrarily shaped interfaces [2]; reduction of the convergence order due to the non-smoothness of the solution across the interfaces, leading to numerical instabilities even for low contrast physical parameters [3]; the jump conditions and the boundary conditions are not incorporated in the schemes, so that the conversion, refraction and diffraction wave phenomena are not correctly described [4], etc.

In addition to the aforementioned difficulties introduced by interfaces, efficiency is another issue that must be dealt with properly. Accuracy and stability may restrict the time-step size to small values, adequate to sub-domains with high wave propagation velocities; in this case, efficiency will be quite poor. This difficulty can be overcome in the case of heterogeneous media by subcycling techniques [5–8], etc., which allow adopting different time-steps for pre-established sub-domains; one such technique is discussed here. In a Boundary Element Method (BEM) context, this situation is even more critical [9]: if small time-step sizes are selected, instabilities may probably occur, and for large time-step sizes, numerical damping is introduced, damaging the accuracy of the analyses.

Stability and accuracy of time-domain BEM algorithms for wave propagation analysis have been the topic of some published papers and refined approaches are now available [10–23]. In the approach developed by Frangi [12], space and time shape functions are not independent as in standard time-domain BEM approaches. Rather, a modified space–time approximation, which represents more accurately the causality of the phenomenon, is employed. Yu et al. [15, 19] achieved more stable time-domain BEM algorithms by introducing, respectively, extra time and space (Galerkin approach) weighting integrals. Three other quite simple and effective schemes presently available are the linear θ method [16–18], the ε scheme and the half-step scheme [10,21]. Many other stabilization schemes can be found in the literature; some are more complex than those mentioned above

D. Soares Jr (✉)
Structural Engineering Department,
Federal University of Juiz de Fora, Cidade Universitária,
CEP 36036-330 Juiz de Fora, MG, Brazil
e-mail: delfim.soares@ufjf.edu.br

(see [20,22], etc.) or are dedicated to minimize one specific source of instability [13,14]. Recently, an efficient and easy to implement stabilized BE formulation was presented by Soares Jr and Mansur [23]. This formulation modifies the BEM time-convolution process, improving the stability and artificial energy dissipation of the method. This procedure is employed here, collaborating to the development of a robust final acoustic–elastodynamic coupling algorithm.

As is well known, stability and accuracy are essential characteristics of any numerical method which is not to be restricted to research topics only. In addition, if a numerical method is to be used by engineers involved in design work, computational efficiency is another required characteristic. Computational efficiency of time-domain BEM for wave propagation analysis has been the subject of research work for the last decades. Truncation strategies were studied in the 1980s, first by Demirel and Wang [24], and later by Mansur and de Lima Silva [25], Soares Jr and Mansur [26] and Carrer and Mansur [27]. Other developments to improve efficiency have been presented by Tröndle and Antes [28], reporting improvements concerning 3D applications, and Tham and Chu [29], describing a parallel algorithm applied to time-domain analyses. In the present work, numerical techniques to truncate the BEM time-convolution process are employed [23,26], improving the efficiency of the coupled approach.

The idea of direct coupling BEM sub-domains by enforcing equilibrium and compatibility of common interface unknowns is reported in the very first BEM texts [30]. The direct coupling idea was soon extended to couple the BEM with other numerical methods, especially the Finite Element Method (FEM), as reported by Zienkiewicz et al. [31] and Brebbia and Georgiou [32], for static problems. Less than a decade afterwards, direct coupling procedures started being employed for many problems, including time-domain wave propagation modelling.

Many algorithms have already been reported concerning BEM–FEM direct coupling for time-domain wave propagation (acoustic, elastic, etc.) analysis [33–39]. In those algorithms, boundary elements either played the rule of a transmitting boundary or (less usual) modelled parts of the domain most suitable to BEM modelling. A good transmitting boundary is in fact a critical requirement in wave propagation analyses of infinite domain problems, because when waves are not properly transmitted to infinity, artificial reflections on the transmitting boundaries may very soon invalidate results.

Most papers dealing with time-domain fluid–solid interactions employ direct coupling to fulfil equilibrium and compatibility conditions on BEM–BEM or BEM–FEM interfaces. Initial papers dealing with BEM–FEM/BEM–BEM coupling for fluid–solid (acoustic–elastodynamic may be a more adequate designation) interaction were concerned with the establishment of a suitable direct coupling approach [35], which could be extended to more complex cases, e.g., non-linear models [39]. More recently, publications concerning stability started appearing, enabling the classical direct coupling algorithms to be applied to more severe situations [40,41]. Direct coupling for solid–solid interaction has also been exhaustively studied, following guidelines similar to those concerning fluid–solid interaction [33,34,38].

In recent years, iterative coupling algorithms have been reported as a promising technique [42]: they may become more accurate, stable, flexible and cheaper than direct coupling procedures. The good performance reported in the literature by iterative coupling for time-independent problems [43,44] encouraged researchers to work out procedures for time-dependent problems. Only a few papers concerning this subject have been published so far, most of them dedicated to BEM–FEM coupling [45–48]. Taking into account time-dependent BEM–BEM iterative coupling, most works are focused on the coupling of boundary element formulations based on transient (the so-called time-domain BEM [9]) and non-transient (the so-called domain BEM [49]) fundamental solutions [50–52]. This work focuses on the iterative coupling of boundary element formulations, all based on transient fundamental solutions. As reported by Soares Jr [42], iterative coupling approaches, besides usually being cheaper than direct coupling algorithms, are quite robust. Therefore, they should be preferred, especially where there are media with quite different physical properties (of the same or different nature).

The present work is mainly concerned with the development of robust and versatile boundary element techniques to numerically model complex wave propagation phenomena, extending the applicability and competitiveness of time-domain boundary element methods. It is organized as follows: in Sect. 2, basic acoustic and elastodynamic governing equations are presented, as well as interacting interface equations. In the sequence, boundary element formulations are briefly described and coupling procedures are discussed (Sects. 3 and 4, respectively). At the end of the paper (Sect. 5), numerical results are presented, illustrating the potentialities of the proposed formulation and the robustness of the developed final coupling algorithm.

2 Governing equations

In the present section, acoustic and elastic wave equations are briefly presented. Each of these wave propagation models is used to model different sub-domains of the global problem. At the end of the section, basic equations concerning the coupling of acoustic and elastodynamic sub-domains are described.

2.1 Acoustic sub-domains

The scalar wave equation is given by

$$p_{,ii} - \ddot{p}/c^2 + s = 0 \tag{1}$$

where $p(X,t)$ stands for hydrodynamic pressure distribution, $s(X,t)$ stands for body source terms and c is the wave propagation velocity. Inferior commas (indicial notation is adopted) and over dots indicate partial space ($p_{,i} = \partial p/\partial x_i$) and time ($\dot{p} = \partial p/\partial t$) derivatives, respectively. The boundary and initial conditions for the problem are given by

(i) Boundary conditions ($t \geq 0$, $X \in \Gamma$ where $\Gamma = \Gamma_1 \cup \Gamma_2$):

$$p(X,t) = \bar{p}(X,t) \quad \text{for } X \in \Gamma_1 \tag{2a}$$

$$q(X,t) = p_{,j}(X,t)\, n_j(X) = \bar{q}(X,t) \quad \text{for } X \in \Gamma_2 \tag{2b}$$

(ii) Initial conditions ($t = 0$, $X \in \Omega$):

$$p(X,0) = \bar{p}_0(X) \tag{3a}$$

$$\dot{p}(X,0) = \dot{\bar{p}}_0(X) \tag{3b}$$

where the prescribed values are indicated by over bars and q represents the flux along the boundary whose unit outward normal vector components are represented by n_j. The boundary of the model is denoted by $\Gamma(\Gamma_1 \cup \Gamma_2 = \Gamma$ and $\Gamma_1 \cap \Gamma_2 = 0)$ and the domain by Ω.

2.2 Elastic sub-domains

The elastic wave equation is given by

$$\left(c_d^2 - c_s^2\right) u_{j,ji} + c_s^2\, u_{i,jj} - \ddot{u}_i + s_i = 0 \tag{4}$$

where $u_i(X,t)$ and $s_i(X,t)$ stand for the displacement and the body force distribution components, respectively. The notation for time and space derivatives employed in Eq. (1) is once again adopted. In Eq. (4), c_d is the dilatational wave velocity and c_s is the shear wave velocity, they are given by: $c_d^2 = (\gamma + 2\mu)/\rho$ and $c_s^2 = \mu/\rho$, where ρ is the mass density of the model and γ and μ are the Lamé's constants. The boundary and initial conditions for the elastodynamic problem are given by

(i) Boundary conditions ($t \geq 0$, $X \in \Gamma$ where $\Gamma = \Gamma_1 \cup \Gamma_2$):

$$u_i(X,t) = \bar{u}_i(X,t) \quad \text{for } X \in \Gamma_1 \tag{5a}$$

$$\tau_i(X,t) = \sigma_{ij}(X,t)\, n_j(X) = \bar{\tau}_i(X,t) \quad \text{for } X \in \Gamma_2 \tag{5b}$$

(ii) Initial conditions ($t = 0$, $X \in \Omega$):

$$u_i(X,0) = \bar{u}_{i0}(X) \tag{6a}$$

$$\dot{u}_i(X,0) = \dot{\bar{u}}_{i0}(X) \tag{6b}$$

where the prescribed values are indicated by over bars and τ_i denotes the traction vector along the boundary (n_j, as indicated previously, stands for the components of the unit outward normal vector and σ_{ij} stands for the components of the stress tensor).

2.3 Acoustic–elastic interacting interfaces

On the acoustic–elastic interface boundaries, the elastic sub-domain normal (normal to the interface) accelerations ($\ddot{u}_N$) are related to the acoustic sub-domain fluxes (q), and the acoustic sub-domain hydrodynamic pressures (p) are related to the elastic sub-domain normal tractions (τ_N). These relations are expressed by the following equations:

$$\ddot{u}_N - (1/\rho)\, q = 0 \tag{7a}$$

$$\tau_N + p = 0 \tag{7b}$$

where in Eqs. (7a, b) the sign of the different sub-domain outward normal directions is taken into account (outward normal vectors on the same interface point are opposite for each sub-domain). In Eq. (7a), ρ is the mass density of the interacting acoustic sub-domain medium.

3 Boundary element formulations

Once the basic governing equations are presented, the discretization of the different sub-domains of the model by boundary element techniques is considered. The first BE formulation focused here is for acoustics and, in Sect. 3.1, the basic BE equations for the solution of acoustic fluids are shown. In the sequence (Sect. 3.2), the BE formulation to model elastodynamic solids is described. Finally, an efficient BE stabilization procedure, applied to both acoustic and elastodynamic models, is presented in Sect. 3.3.

3.1 Acoustic formulation

The integral equation related to acoustic models is given by:

$$\begin{aligned} c(\xi)\, p(\xi,t) = &\int_\Gamma \int_0^{t+} p^*(X,t;\xi,\tau) q(X,\tau)\, d\tau\, d\Gamma(X) \\ &- \int_\Gamma \int_0^{t+} q^*(X,t;\xi,\tau) p(X,\tau)\, d\tau\, d\Gamma(X) \\ &+ s(X,t;\xi,\tau) \end{aligned} \tag{8}$$

where $c(\xi)$ depends on geometric aspects and the terms $p^*(X,t;\xi,\tau)$ and $q^*(X,t;\xi,\tau)$ represent the fundamental potential (hydrodynamic pressure) and flux, respectively (X is the field point and ξ is the source point; the distance between X and ξ is given by r). $s(X,t;\xi,\tau)$ stands for possible domain integral contributions (initial conditions or/and body forces).

Taking into account the fundamental solutions of the problem, Eq. (8) can be re-written as follows:

$$c\,p = \int_{\Gamma} \left(\int_0^{t+} L H q \, d\tau \right) d\Gamma - \int_{\Gamma} (\partial r/\partial n) \left(\oint_0^{t+} r L^3 H p \, d\tau \right) d\Gamma + s' \tag{9}$$

where H (scaled Heaviside function) and L are given by

$$H = c/(2\pi)\, H(c(t-\tau) - r) \tag{10a}$$

$$L = (c^2(t-\tau)^2 - r^2)^{-1/2} \tag{10b}$$

and the symbol $\oint$ on the second term on the right-hand side of Eq. (9) stands for the finite part of an integral. Following Hadamard [53], this operation can be written as

$$\oint_0^{t+} r L^3 H p \, d\tau = c/(2\pi) \lim_{\tau \to t - r/c} \left(\int_0^{t+} r L^3 p \, d\tau - (1/c) L p \right) \tag{11}$$

Adopting the following space–time approximations for the variables of the model (η and ϕ are space and time interpolation functions, respectively, related to a boundary node j and a discrete time m):

$$p(X,t) = \sum_{j=1}^{J} \sum_{m=1}^{M} \phi_p^m(t)\, \eta_p^j(X)\, p_j^m \tag{12a}$$

$$q(X,t) = \sum_{j=1}^{J} \sum_{m=1}^{M} \phi_q^m(t)\, \eta_q^j(X)\, q_j^m \tag{12b}$$

the following system of equations can be obtained, by substituting Eqs. (12a, b) into Eq. (9) and considering proper numerical treatment:

$$\mathbf{C}\mathbf{P}^n = \mathbf{G}^1\mathbf{Q}^n - \mathbf{H}^1\mathrm{P}^n + \mathbf{R}^n + \mathbf{S}^n \tag{13a}$$

$$\mathbf{R}^n = \sum_{l=1}^{n-1} \left(\mathbf{G}^{n-l+1}\mathbf{Q}^l - \mathbf{H}^{n-l+1}\mathbf{P}^l \right) \tag{13b}$$

where $\mathbf{C}$, $\mathbf{G}$ and $\mathbf{H}$ are influence matrices; $\mathbf{R}^n$ is a vector standing for the time convolution process; $\mathbf{S}^n$ is a vector related to domain integrals and $\mathbf{P}^n$ and $\mathbf{Q}^n$ are pressure and flux vectors, respectively, at the discrete time n. After introducing the boundary conditions of the model, the system of Eqs. (13a, b) can be solved for pressures and fluxes, at each time t_n. For more details concerning the acoustic BE formulation, the reader is referred to [9,54,55].

In the present work, linear spatial interpolation functions are considered (η_p and η_q), as well as linear temporal interpolation functions for hydrodynamic pressures (ϕ_p) and piecewise constant temporal interpolation functions for hydrodynamic fluxes (ϕ_q).

3.2 Elastodynamic formulation

The integral equation related to elastodynamic models is given by

$$c_{ik}(\xi) u_{ik}(\xi,t) = \int_{\Gamma} \int_0^{t+} u_{ik}^*(X,t;\xi,\tau)\tau_k(X,\tau) d\tau d\Gamma(X) - \int_{\Gamma} \int_0^{t+} \tau_{ik}^*(X,t;\xi,\tau) u_k(X,\tau) d\tau \, d\Gamma(X) + s_i(X,t;\xi,\tau) \tag{14}$$

where the terms $u_{ik}^*(X,t;\xi,\tau)$ and $\tau_{ik}^*(X,t;\xi,\tau)$ represent the dynamic fundamental displacement and traction, respectively (the remainder terms of Eq. (14) are analogous to the ones depicted in Eq. (8)).

Taking into account the fundamental solutions of the problem, Eq. (14) can be re-written as follows:

$$\begin{aligned} c_{ik}\, u_k = &- \int_{\Gamma} F_{ik} \left(\int_0^{t+} L_d^{-1} H_d \tau_k \, d\tau \right) d\Gamma \\ &- \int_{\Gamma} E_{ik} \left(\int_0^{t+} L_d N_d H_d \tau_k \, d\tau \right) d\Gamma \\ &+ \int_{\Gamma} D_{ik} \left(\oint_0^{t+} r L_d^3 H_d u_k \, d\tau \right) d\Gamma \\ &+ \int_{\Gamma} B_{ik} \left(\int_0^{t+} L_d N_d H_d u_k \, d\tau \right) d\Gamma \\ &+ \int_{\Gamma} F_{ik} \left(\int_0^{t+} L_s^{-1} H_s \tau_k \, d\tau \right) d\Gamma \\ &+ \int_{\Gamma} E_{ik} \left(\int_0^{t+} L_s N_s H_s \tau_k \, d\tau \right) d\Gamma \\ &- \int_{\Gamma} D_{ik} \left(\oint_0^{t+} r L_s^3 H_s u_k \, d\tau \right) d\Gamma \\ &- \int_{\Gamma} B_{ik} \left(\int_0^{t+} L_s N_s H_s u_k \, d\tau \right) d\Gamma \end{aligned}$$

$$+\int_{\Gamma}\delta_{ik}\left(\int_{0}^{t+}L_s H_s \tau_k\, d\tau\right) d\Gamma$$

$$-\int_{\Gamma}A_{ik}\left(\oint_{0}^{t+} r L_s^3 H_s u_k\, d\tau\right) d\Gamma + s_i' \tag{15}$$

where H_w (scaled Heaviside function), L_w and N_w are given by (the subscript w can be conveniently substituted by s or by d in order to represent the contribution of the secondary or the primary wave, respectively):

$$H_w = 1/(2\pi\rho\, c_w)\, H(c_w(t-\tau)-r) \tag{16a}$$

$$L_w = \left(c_w^2(t-\tau)^2 - r^2\right)^{-1/2} \tag{16b}$$

$$N_w = 2c_w^2(t-\tau)^2 - r^2 \tag{16c}$$

and the tensors A_{ik}, B_{ik}, D_{ik}, E_{ik} and F_{ik} are defined as (δ_{ik} is the Kronecker delta):

$$A_{ik} = \gamma\, n_k r_{,i} + \delta_{ik}\mu\, (\partial r/\partial n) + \mu\, n_i r_{,k} \tag{17a}$$

$$B_{ik} = -2\mu\, r^{-3}\left(\delta_{ik}(\partial r/\partial n) + n_i r_{,k} + n_k r_{,i} - 4(\partial r/\partial n) r_{,i} r_{,k}\right) \tag{17b}$$

$$D_{ik} = -\lambda\, n_k r_{,i} - 2\mu\, (\partial r/\partial n) r_{,i} r_{,k} \tag{17c}$$

$$E_{ik} = -r^{-2} r_{,i} r_{,k} \tag{17d}$$

$$F_{ik} = r^{-2}\delta_{ik} \tag{17e}$$

In Eq. (15), the finite part integral is to be interpreted as:

$$\oint_{0}^{t+} r L_w^3 H_w u_k\, d\tau = 1/(2\pi\rho\, c_w) \lim_{\tau\to t-r/c_w}\left(\int_{0}^{t+} r L_w^3 u_k\, d\tau - (1/c_w) L_w u_k\right) \tag{18}$$

Analogously as presented in the previous sub-section, adopting the following space–time approximations for the variables of the model:

$$u_k(X,t) = \sum_{j=1}^{J}\sum_{m=1}^{M}\phi_u^m(t)\,\eta_u^j(X)\,u_{kj}^m \tag{19a}$$

$$\tau_k(X,t) = \sum_{j=1}^{J}\sum_{m=1}^{M}\phi_\tau^m(t)\,\eta_\tau^j(X)\,\tau_{kj}^m \tag{19b}$$

the following system of equations can be obtained:

$$\mathbf{C}\mathbf{U}^n = \mathbf{G}^1\mathbf{T}^n - \mathbf{H}^1\mathbf{U}^n + \mathbf{R}^n + \mathbf{S}^n \tag{20a}$$

$$\mathbf{R}^n = \sum_{l=1}^{n-1}\left(\mathbf{G}^{n-l+1}\mathbf{T}^l - \mathbf{H}^{n-l+1}\mathbf{U}^l\right) \tag{20b}$$

where $\mathbf{C}$, $\mathbf{G}$ and $\mathbf{H}$ are, once again, influence matrices; $\mathbf{R}^n$ stands for the time convolution process; $\mathbf{S}^n$ is related to domain integrals and $\mathbf{U}^n$ and $\mathbf{T}^n$ are displacement and traction vectors, respectively, at the discrete time n. After introducing the boundary conditions of the model, the system of Eqs. (20a, b) can be solved for displacements and tractions, at each time t_n. For more details concerning the present elastodynamic BE formulation, the reader is referred to [9,54,56].

In the present work, linear spatial interpolation functions are considered (η_u and η_τ), as well as linear temporal interpolation functions for displacements (ϕ_u) and piecewise constant temporal interpolation functions for tractions (ϕ_τ).

3.3 Stabilized formulation

After introducing the boundary conditions in Eqs. (13a, b) or (20a, b), the following expressions are obtained:

$$\mathbf{A}\mathbf{X}^n = \mathbf{B}\mathbf{Y}^n + \mathbf{R}^n + \mathbf{S}^n \tag{21a}$$

$$\mathbf{R}^n = \sum_{l=1}^{n-1}\left(\mathbf{G}^{n-l+1}\mathbf{V}_{\mathrm{G}}^l - \mathbf{H}^{n-l+1}\mathbf{V}_{\mathrm{H}}^l\right) \tag{21b}$$

where, as usual in time-domain BEM, the entries of $\mathbf{X}^n$ are unknown variables at boundary nodes at discrete time t_n, while the entries of vector $\mathbf{Y}^n$ are the according known nodal values. Matrices $\mathbf{A}$ and $\mathbf{B}$ are obtained from the combination of matrices $\mathbf{C}+\mathbf{H}^1$ and $\mathbf{G}^1$, taking into account, as well, the prescribed boundary conditions. Vectors $\mathbf{V}_{\mathrm{G}}$ and $\mathbf{V}_{\mathrm{H}}$ stand for acoustic fluxes or elastodynamic tractions and acoustic pressures or elastodynamic displacements, respectively. The time stepping procedure indicated by Eqs. (21a, b) requires convolutions ($l = 1, 2, \ldots, n-1$) to be carried out for $n = 1, 2, \ldots, N$, where the final time is $T_N = N\Delta t$, Δt being the time step.

In order to achieve an efficient stabilized boundary element formulation, the present work modifies the BEM convolution vector (Eq. (21b)), introducing a stabilization parameter into the recent-in-time convolution operations and a time-truncation procedure to compute the distant-in-time convolution contributions. No modification is introduced in the evaluation of the standard BEM matrices $\mathbf{H}^n$ and $\mathbf{G}^n$, only their manipulation along the time-convolution process is modified.

Taking into account the above described time-convolution modification, Eqs. (21a, b) can be re-written as follows:

$$\bar{\mathbf{A}}\mathbf{X}^n = \bar{\mathbf{B}}\mathbf{Y}^n + \bar{\mathbf{R}}^n + \hat{\mathbf{R}}^n + \mathbf{S}^n \tag{22a}$$

$$\bar{\mathbf{R}}^n = \sum_{l=n-L+1}^{n-1}\left\{\mathbf{G}^{n-l+1}\sum_{k=-1}^{1-\delta_{l,n-1}}\left[J(\lambda,k)\mathbf{V}_{\mathrm{G}}^{l+k}\right] - \mathbf{H}^{n-l+1}\sum_{k=-1}^{1-\delta_{l,n-1}}\left[J(\lambda,k)\mathbf{V}_{\mathrm{H}}^{l+k}\right]\right\} \tag{22b}$$

$$\hat{\mathbf{R}}^n = \sum_{k=1}^{m} \left\{ \mathbf{G}_k \sum_{l=1}^{n-L} \left[I(n-l+1,k)\mathbf{V}_{\mathrm{G}}^l \right] - \mathbf{H}_k \sum_{l=1}^{n-L} \left[I(n-l+1,k)\mathbf{V}_{\mathrm{H}}^l \right] \right\} \tag{22c}$$

where $J(\cdot)$ and $I(\cdot)$ are scalar functions; they define stabilization coefficients and interpolation parameters, respectively. Matrices $\bar{\mathbf{A}}$ and $\bar{\mathbf{B}}$ are obtained from the combination of matrices $\mathbf{C}+\mathbf{H}^1+J(\lambda,1)\mathbf{H}^2$ and $\mathbf{G}^1+J(\lambda,1)\mathbf{G}^2$, taking into account the prescribed boundary conditions of the problem ($0 \le \lambda \le 1$ is a stabilization parameter; for $\lambda = 0$ standard formulation is obtained). $\bar{\mathbf{R}}^n$ is the vector related to the recent-in-time convolution process (it represents the time history from t_{n-L+1} up to t_{n-1}, where L is a parameter which defines the truncation point of the BEM convolution process) and $\hat{\mathbf{R}}^n$ is a truncated BEM convolution vector. This truncated approach consists of evaluating the matrices $\mathbf{H}^{n-l+1}$ and $\mathbf{G}^{n-l+1}$ by interpolation, based on a few m-calculated matrices $\mathbf{H}_k$ and $\mathbf{G}_k$ ($k = 1, 2, \ldots, m$), computed at appropriate discrete times T_k ($T_L \le T_k \le T_N$, where T_L is the time limit after which the approximations take place). The integer m is an input parameter to the approximated convolution analysis and it indicates the number of key time-points (T_k) to be used in the interpolation procedure (the interpolations will occur within the interlude of these key time-points).

There are several stabilization and interpolation procedures that might be chosen to specify $J(\cdot)$ and $I(\cdot)$; for a detailed discussion, the reader is referred to [23,26]. In the present work, the following expressions are considered:

$$J(\lambda,k) = \tfrac{1}{2}\lambda k^2 + (1-k^2)(1-\lambda) \tag{23a}$$

$$I(j,k) = \frac{j\Delta t - T_{k-1}}{T_k - T_{k-1}} \times \left[H(j\Delta t - T_{k-1})\ H(T_k - j\Delta t) \right] (1-\delta_{k,1}) + \frac{T_{k+1} - j\Delta t}{T_{k+1} - T_k} \times \left[H(j\Delta t - T_k)\ H(T_{k+1} - j\Delta t) \right] (1-\delta_{k,m}) \tag{23b}$$

which adopt a simple linear combination (based on the λ parameter) of three consecutive time-step results for the stabilization of the standard boundary element formulation (Eq. (23a)) and consider simple linear interpolation between the m selected interpolation time-points (multi-linear interpolation algorithm) for the truncation of the time-convolution process (Eq. (23b)).

4 Coupling procedures

In the current section, the coupling of the BE formulations previously presented is considered. This work employs iterative coupling procedures to take into account the interaction of the different BE formulations presented (each BE formulation models a specific sub-domain of the fluid–solid coupled problem). As has been shown [42], iterative coupling is a very versatile procedure. It allows independent analyses of each sub-domain of the global model: interaction effects are carried out by boundary values, which are iteratively updated along the common interfaces.

In the iterative coupling of the acoustic and the elastodynamic BE formulations, natural boundary conditions are prescribed on the common interfaces, for each sub-domain. The displacements evaluated at the sub-domains modelled by the elastodynamic formulation are used to obtain the fluxes (prescribed interface boundary condition) for the sub-domains modelled by the acoustic formulation; the pressures evaluated at the sub-domains modelled by the acoustic formulation are used to obtain the tractions (prescribed interface boundary condition) for the sub-domains modelled by the elastodynamic formulation. Concisely, each sub-domain is analysed separately ($\mathbf{U}$ and $\mathbf{P}$ are evaluated at each iterative step) and the interface relations $\mathbf{U} \rightarrow \mathbf{Q}$ and $\mathbf{P} \rightarrow \mathbf{T}$ are iteratively considered until convergence is achieved.

In this section, first some special procedures, which are used in conjunction with the adopted iterative coupling, are discussed (Sects. 4.1, 4.2 and 4.3) and, next, the final coupling algorithm is presented (Sect. 4.4).

4.1 Stabilized iterative coupling

In the present iterative coupling procedure, a relaxation parameter α is considered, which relates the recent BEM results (${}^{(k+\alpha)}\mathbf{V}$) with the results of the previous iterative step (${}^{(k)}\mathbf{V}$) and the final results (${}^{(k+1)}\mathbf{V}$) at the current iterative step. Considering a generic variable $\mathbf{V}$, the adoption of a relaxation parameter α can be described as follows:

$${}^{(k+1)}\mathbf{V} = (\alpha)\,{}^{(k+\alpha)}\mathbf{V} + (1-\alpha)\,{}^{(k)}\mathbf{V} \tag{24}$$

As has been reported [42–48], the introduction of a relaxation parameter α is extremely important in order to ensure or/and speed up the convergence of the iterative coupling process.

4.2 Different sub-domain discretizations

In order to consider different time-steps in each sub-domain, interpolation/extrapolation procedures along time are here considered. In the present work, the temporal interpolation/extrapolation procedures are based on the BEM time interpolation functions (piecewise constant $\phi_q(t)$ and $\phi_\tau(t)$ and linear $\phi_p(t)$ and $\phi_u(t)$), as depicted in Figure 1 (Fig. 1 describes the calculus of some time-interpolated/extrapolated variables which are important in the context of the final coupling algorithm presented in Sect. 4.4).

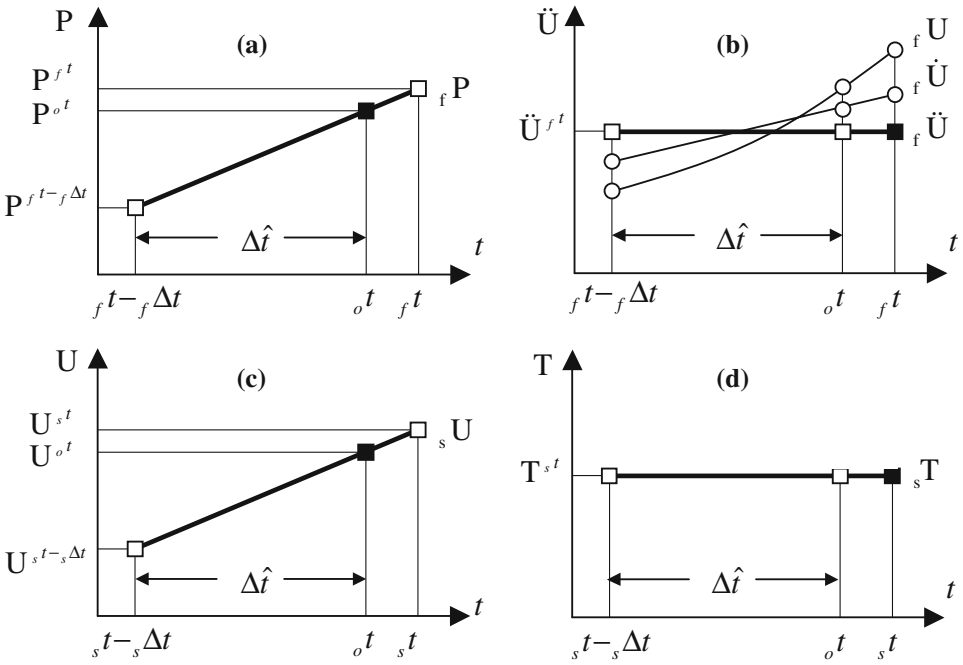

Fig. 1 Time interpolation/extrapolation procedures: **a** fluid-domain interpolation: $\mathrm{P}^{o\,t} = \mathrm{P}^{f\,t}(\Delta\hat{t}/{}_f\Delta t) + \mathrm{P}^{f\,t-{}_f\Delta t}(1-\Delta\hat{t}/{}_f\Delta t)$, **b** fluid-domain extrapolation: $\ddot{\mathrm{U}}^{f\,t} = \ddot{\mathrm{U}}^{o\,t}$, **c** solid-domain interpolation: $\mathrm{U}^{o\,t} = \mathrm{U}^{s\,t}(\Delta\hat{t}/{}_s\Delta t) + \mathrm{U}^{s\,t-{}_s\Delta t}(1-\Delta\hat{t}/{}_s\Delta t)$, **d** solid-domain extrapolation: $\mathrm{T}^{s\,t} = \mathrm{T}^{o\,t}$

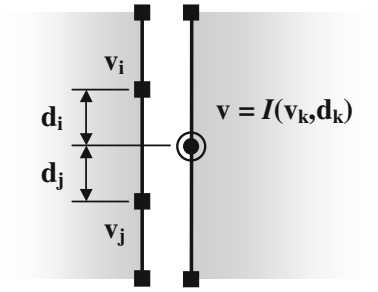

Fig. 2 Space interpolation procedures: interpolation scheme of $\mathbf{v}_k$ values in order to obtain $\mathbf{v}$ (linear interpolation: $\mathbf{v} = (\mathbf{v}_\mathrm{i}\mathbf{d}_\mathrm{j} + \mathbf{v}_\mathrm{j}\mathbf{d}_\mathrm{i})/(\mathbf{d}_\mathrm{j} + \mathbf{d}_\mathrm{i})$)

Spatial interpolation procedures may also be adopted in order to consider independent BEM meshes. In Fig. 2, for instance, a simple scheme is shown to evaluate a sub-domain nodal value by means of the nodal values of the adjacent sub-domain, when there is not a direct connection among the nodes (one should observe that linear spatial interpolation functions are considered here).

Using space/time interpolation/extrapolation procedures, optimal BE modelling in each sub-domain may be achieved, which is very important regarding flexibility, efficiency, accuracy and stability.

4.3 Interface treatment

Equations (7a,b) are employed in order to couple acoustic fluid and elastodynamic solid sub-domains; however, since the elastodynamic BE formulation usually does not evaluate accelerations, Eq. (7a) must be adapted.

In order to relate the fluxes (${}_f\mathbf{Q}$, where subscript f stands for fluid sub-domain) of the acoustic BE formulation with the displacements (${}_s\mathbf{U}$, where subscript s stands for solid sub-domain) of the elastodynamic BE formulation (adaptation of relation (7a)), the characteristics of the time interpolation function $\phi_q(t)$ is once again taken into account. Since the present work adopts $\phi_q(t)$ as being piecewise constant, an equivalent displacement ${}_f\mathbf{U}^t$ can be obtained from the equivalent acceleration ${}_f\ddot{\mathbf{U}}^t$ by time integration, as follows:

$$
\begin{aligned}
{}_f\mathbf{U}^t \;=\; & {}_f\mathbf{U}^{t_i} + {}_f\dot{\mathbf{U}}^{t_i}\,(t-t_i) \\
& + {}_f\ddot{\mathbf{U}}^t\,(t-t_i)^2/2, \quad \forall t \in \left(t_i;\; t_i + {}_f\Delta t\right]
\end{aligned}
\tag{25}
$$

where ${}_f\Delta t$ is the time-step of the acoustic BE formulation. According to Eq. (25), along each time-step ${}_f\Delta t$, the equivalent displacements, velocities and accelerations (acoustic BE formulation) have parabolic, linear and piecewise constant behavior, respectively (see Fig. 1b). It is important to note that Eq. (25) is equivalent to the Newmark method [57], adopting the parameters: $N_1 = 1.00$ and $N_2 = 0.50$ (the classical Newmark's trapezoidal rule is given by: $N_1 = 0.50$ and $N_2 = 0.25$).

Finally, a relation between ${}_s\mathbf{U}^t$ and ${}_f\mathbf{Q}^t$ can be numerically established as follows (analogously to Eq. (7a)): ${}_f\mathbf{U}^t_N$ can be related to ${}_s\mathbf{U}^t_N$ and, in the sequence, ${}_f\mathbf{Q}^t$ can be related to ${}_f\mathbf{U}^t_N$ by taking into account Eq. (25) (calculus of ${}_f\ddot{\mathbf{U}}^t_N$) and relation ${}_f\ddot{\mathbf{U}}^t_N = (1/{}_f\rho)\,{}_f\mathbf{Q}^t$ (more details are given in Sect. 4.4).

4.4 Final coupling algorithm

The basic steps of the developed acoustic–elastodynamic coupling algorithm are presented below. In the algorithm that follows, a reference time-step (${}_o\Delta t$) is introduced, which is the algorithm time-marching step: ${}_o\Delta t$ must be smaller (or equal) than all the sub-domain time-steps considered in the model, hence all sub-domain time-marching schemes can be properly considered (${}_o\Delta t$ is usually selected equal to the smallest time-step in the analysis). As one will observe, all aspects previously discussed in the present section are integrated in this final coupling algorithm.

Final coupling algorithm:

(1) *Initial calculations*
- (1.1) *Time marching initialisation*
  - (1.1.1) *Time-steps for each sub-domain are selected* (${}_f\Delta t$ *and* ${}_s\Delta t$)
  - (1.1.2) *A reference time-step is selected* (${}_o\Delta t$, *where* ${}_o\Delta t \leq {}_f\Delta t$ *and* ${}_o\Delta t \leq {}_s\Delta t$)
  - (1.1.3) *Initial time attributions are considered:* ${}_ft = {}_f\Delta t$; ${}_st = {}_s\Delta t$ *and* ${}_ot = 0$
- (1.2) *BEM standard initial calculations are considered, (e.g., matrices* ${}_{f/s}\bar{\mathbf{A}}, {}_{f/s}\bar{\mathbf{B}}$ *etc.)*
- (1.3) *Initial prescribed values are chosen at common interface surfaces (e.g.,* ${}^{(0)}_{s}\mathbf{T} = \mathbf{0}$)

(2) *Time-step loop*
- (2.1) *Beginning of evaluations at each time step*
  - (2.1.1) *Update* ${}_ot = {}_ot + {}_o\Delta t$
  - (2.1.2) *If* ${}_ot > {}_ft$ *: update* ${}_ft = {}_ft + {}_f\Delta t$ *and evaluate vectors* ${}_f\bar{\mathbf{R}}^{ft}, {}_f\hat{\mathbf{R}}^{ft}$ *and* ${}_f\mathbf{S}^{ft}$
  - (2.1.3) *If* ${}_ot > {}_st$: *update* ${}_st = {}_st + {}_s\Delta t$ *and evaluate vectors* ${}_s\bar{\mathbf{R}}^{st}, {}_s\hat{\mathbf{R}}^{st}$ *and* ${}_s\mathbf{S}^{st}$
- (2.2) *Iterative loop*
  - (2.2.1) *Elastodynamic BE analysis: obtain* ${}^{(k+\alpha)}_{s}\mathbf{U}^{st}$ (Sects. 3.2 *and* 3.3)
  - (2.2.2) *Adoption of a relaxation parameter* (Eq. (24)): ${}^{(k+1)}_{s}\mathbf{U}^{st} = (\alpha){}^{(k+\alpha)}_{s}\mathbf{U}^{st} + (1-\alpha){}^{(k)}_{s}\mathbf{U}^{st}$
  - (2.2.3) *From* ${}^{(k+1)}_{s}\mathbf{U}^{st}$ *obtain* ${}^{(k+1)}_{s}\mathbf{U}^{ot}$ (*time interpolation*—Fig. 1c)
  - (2.2.4) *From* ${}^{(k+1)}_{s}\mathbf{U}^{ot}$ *obtain* ${}^{(k+1)}_{f}\mathbf{U}^{ot}_{N}$ (*space interpolation*—Fig. 2)
  - (2.2.5) *From* ${}^{(k+1)}_{f}\mathbf{U}^{ot}_{N}$ *obtain* ${}^{(k+1)}_{f}\ddot{\mathbf{U}}^{ot}_{N}$ (Eq. (25)): $${}^{(k+1)}_{f}\ddot{\mathbf{U}}^{ot}_{N} = (2/\Delta\hat{t}^2)\left({}^{(k+1)}_{f}\mathbf{U}^{ot}_{N} - {}_f\mathbf{U}_N^{{}^ft-{}_f\Delta t}\right) - (2/\Delta\hat{t})\left({}_f\dot{\mathbf{U}}_N^{{}^ft-{}_f\Delta t}\right)$$
  - (2.2.6) *From* ${}^{(k+1)}_{f}\ddot{\mathbf{U}}^{ot}_{N}$ *obtain* ${}^{(k+1)}_{f}\ddot{\mathbf{U}}^{ft}_{N}$ (*time extrapolation*—Fig. 1b)
  - (2.2.7) *From* ${}^{(k+1)}_{f}\ddot{\mathbf{U}}^{ft}_{N}$ *obtain* ${}^{(k+1)}_{f}\mathbf{Q}^{ft}$ (Eq. (7a))
  - (2.2.8) *Acoustic BE analysis*: *obtain* ${}^{(k+1)}_{f}\mathbf{P}^{ft}$ (Sects. 3.1 *and* 3.3)
  - (2.2.9) *From* ${}^{(k+1)}_{f}\mathbf{P}^{ft}$ *obtain* ${}^{(k+1)}_{f}\mathbf{P}^{ot}$ (*time interpolation*—Fig. 1a)
  - (2.2.10) *From* ${}^{(k+1)}_{f}\mathbf{P}^{ot}$ *obtain* ${}^{(k+1)}_{f}\mathbf{T}^{ot}_{N}$ (Eq. (7b))
  - (2.2.11) *From* ${}^{(k+1)}_{f}\mathbf{T}^{ot}_{N}$ *obtain* ${}^{(k+1)}_{s}\mathbf{T}^{ot}$ (*space interpolation*—Fig. 2)
  - (2.2.12) *From* ${}^{(k+1)}_{s}\mathbf{T}^{ot}$ *obtain* ${}^{(k+1)}_{s}\mathbf{T}^{st}$ (*time extrapolation*—Fig. 1d)
  - (2.2.13) *Check for convergence and go to step* (2.2) *or* (2.3)
- (2.3) *Updating* (*and printing*) *of BE results*
  - (2.3.1) *If* ${}_ot + {}_o\Delta t > {}_st$ *: update* (*and print*) *elastodynamic BE results*

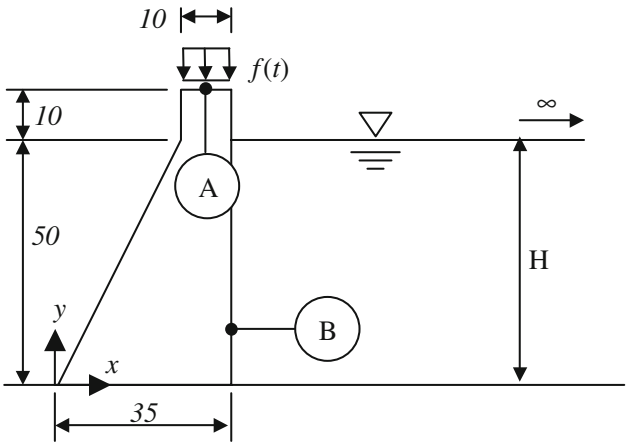

Fig. 3 Sketch of the dam and storage-lake coupled system (point A: $x = 30$ m, $y = 60$ m; point B: $x = 35$ m, $y = 10$ m)

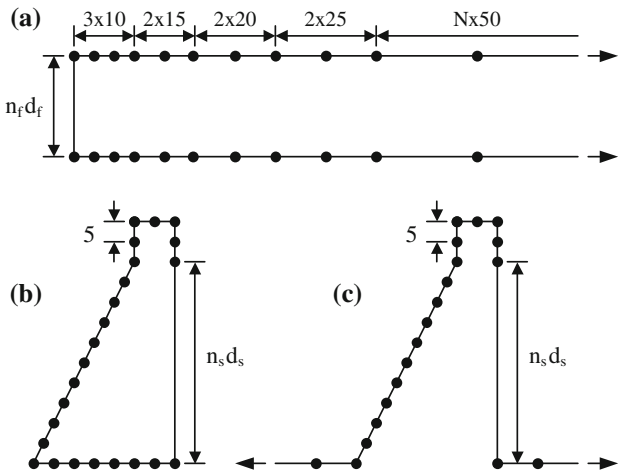

Fig. 4 Sketch of the BEM meshes: **a** storage-lake (opened-domain), **b** dam (closed-domain), and **c** dam (opened-domain) spatial discretizations

(2.3.2) *If* $_{o}t + {}_{o}\Delta t > {}_{f}t$: *update* (*and print*) *acoustic BE results, including*:

$$ {}_{f}\mathbf{U}_{N}^{f t} = {}_{f}\mathbf{U}_{N}^{f t-{}_{f}\Delta t} + \left({}_{f}\Delta t\right)_{f}\dot{\mathbf{U}}_{N}^{f t-{}_{f}\Delta t} + \left({}_{f}\Delta t^{2}/2\right)_{f}\ddot{\mathbf{U}}_{N}^{f t} $$

$$ {}_{f}\dot{\mathbf{U}}_{N}^{f t} = {}_{f}\dot{\mathbf{U}}_{N}^{f t-{}_{f}\Delta t} + \left({}_{f}\Delta t\right)_{f}\ddot{\mathbf{U}}_{N}^{f t} $$

(2.4) *Check* $_{o}t$ *and go to step* (2) *or* (3)

(3) *End of calculation*

Table 1 Cases of analysis considering different time and space (interface) discretizations for the dam–reservoir system

Case	Solid		Fluid	
	d (m)	Δt (s)	d (m)	Δt (s)
1	5.0	0.0030	5.0	0.0030
2	5.0	0.0030	2.5	0.0015
3	5.0	0.0030	10.0	0.0060
4	5.0	0.0015	5.0	0.0030
5	5.0	0.0015	5.0	0.0060
6	2.5	0.0015	2.5	0.0015
7	2.5	0.0030	2.5	0.0015
8	10.0	0.0060	10.0	0.0060
9	10.0	0.0015	10.0	0.0075

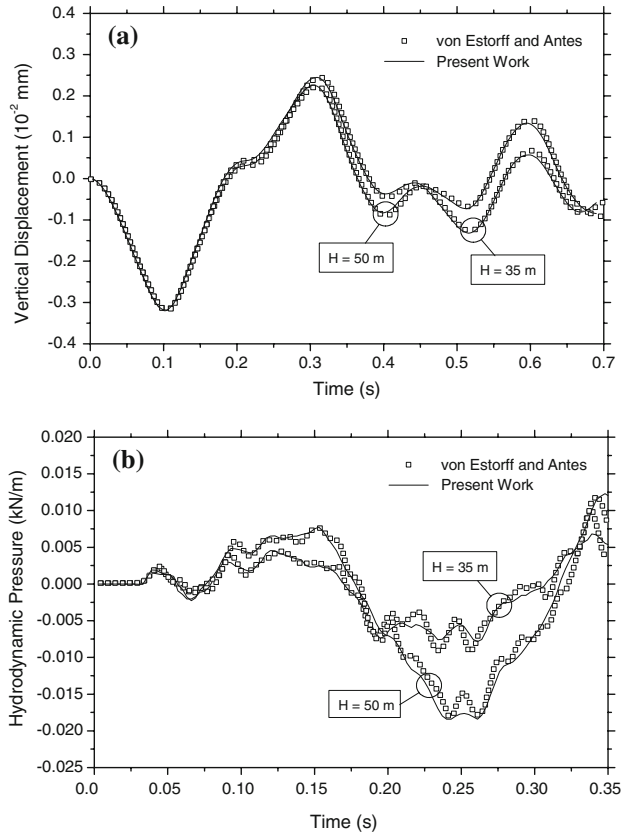

Fig. 5 Case 1 time history results for $H = 35$ m and $H = 50$ m: **a** vertical displacements at point A, **b** hydrodynamic pressures at point B

5 Numerical applications

Two numerical examples are considered in the present section. The first one deals with a loaded dam retaining the water of a semi-infinite storage-lake. The second one is concerned with the analysis of a solid wall adjacent to a closed-domain fluid. For all examples presented here, the reference time-step is selected equal to the smallest time-step in the analysis and a relaxation parameter $\alpha = 0.5$ is adopted.

It is important to observe that, for several fluid–solid interaction analyses, including the present ones, iterative coupling algorithms do not converge when the introduction of the relaxation parameter is disregarded (for details concerning convergence aspects of time-domain iterative BEM–BEM coupling algorithms, one is referred to [42,50]). In fact, usually acoustic–elastodynamic coupled systems are quite difficult to model, in spite of the coupling procedures adopted, as has been reported by Yu et al. [41], Czygan [58] and Soares Jr et al. [47].

5.1 Dam–reservoir system

In this first example, a dam–reservoir system, as depicted in Fig. 3, is analyzed [35]. The structure is subjected to a

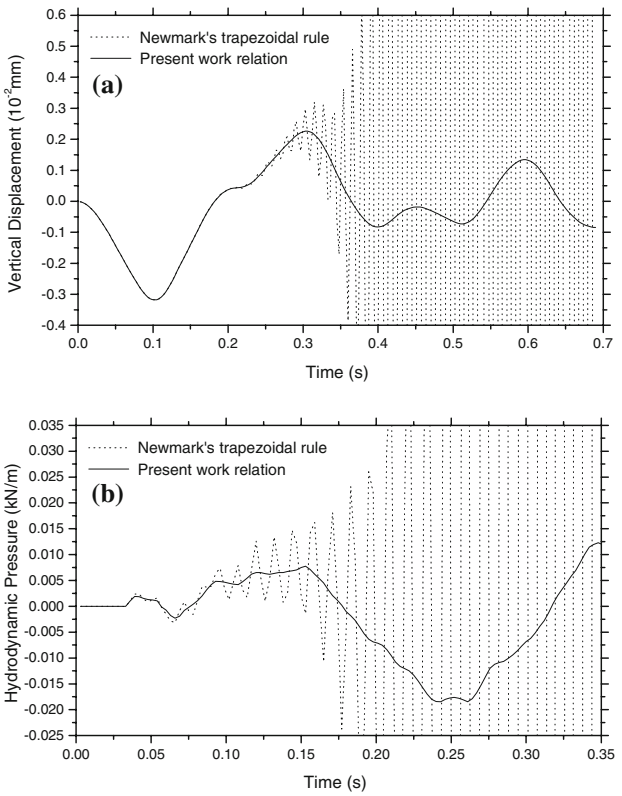

Fig. 6 Case 1 time history results ($H = 50$ m) considering different interface relations ($_{s}\mathbf{U} \rightarrow {}_{f}\ \mathbf{Q}$) for the coupling of acoustic and elastodynamic BE formulations (Eq. (25)): **a** vertical displacements at point A, **b** hydrodynamic pressures at point B

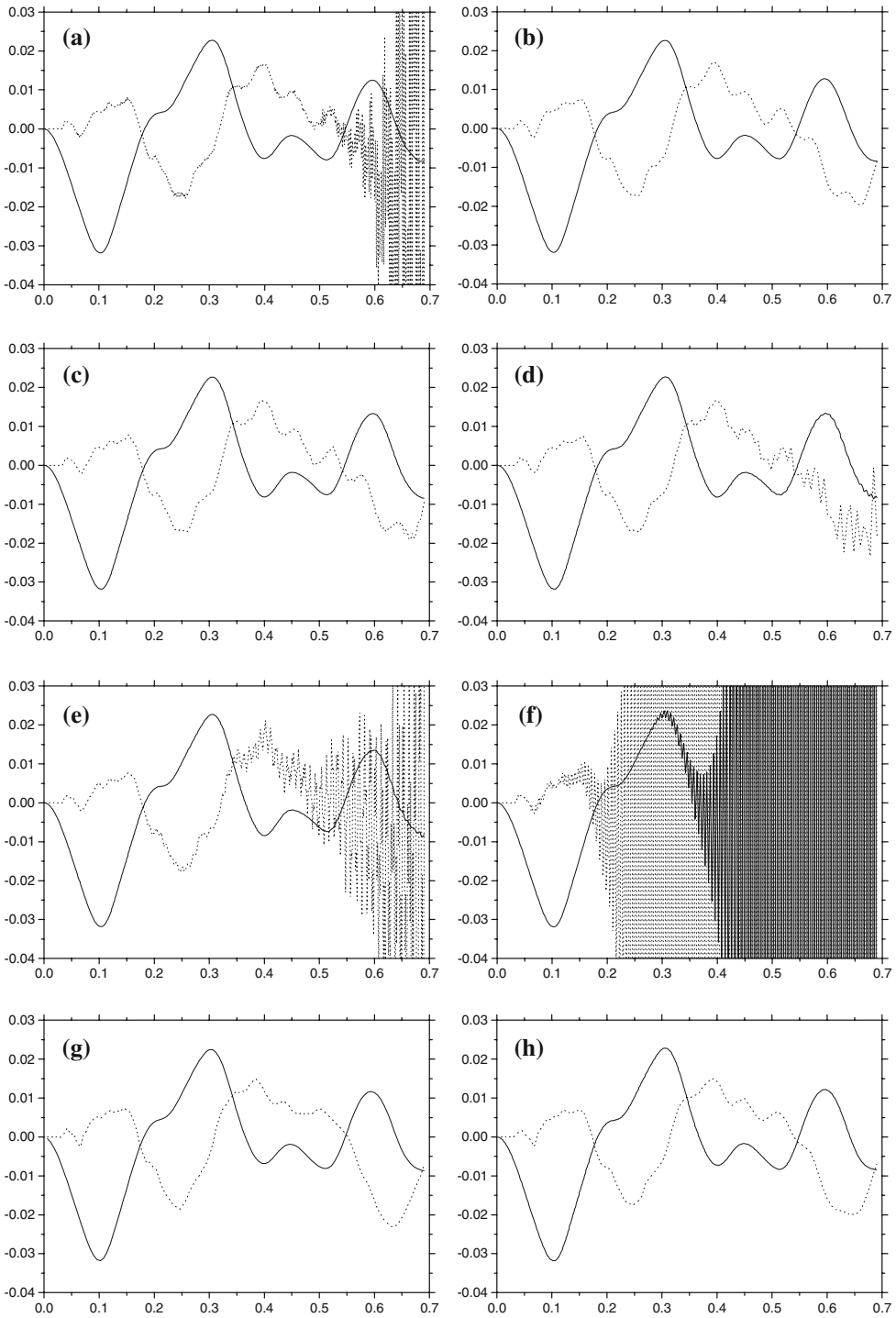

Fig. 7 Scaled vertical displacement (*solid line*) and hydrodynamic pressure (*dot line*) time history results at points A and B, respectively: **a** case 2, **b** case 3, **c** case 4, **d** case 5, **e** case 6, **f** case 7, **g** case 8, **h** case 9

sinusoidal distributed vertical load on its crest, acting with an angular frequency $w = 18$ rad/s. The material properties of the dam are: Poisson's ratio $\nu = 0.25$; Young's modulus $E = 3.437 \times 10^6$ kN/m^2; mass density ρ = 2,000 kg/m^3. The adjacent fluid is characterized by a mass density ρ = 1,000 kg/m^3 and a wave velocity $c = 1,436$ m/s.

The spatial discretization adopted for the storage-lake is depicted in Fig. 4a (for $x > 185$ m, the mesh is expanded by equal-sized boundary elements with length 50 m). The dam spatial discretization is depicted in Fig. 4b. For the fluid–solid common interface, different spatial discretizations are considered, as described in Table 1 (it is important to note that equal-sized elements are always applied along the common interface, for each sub-domain). The different time-steps adopted, in each sub-domain, are also presented in Table 1, according to the case of analysis.

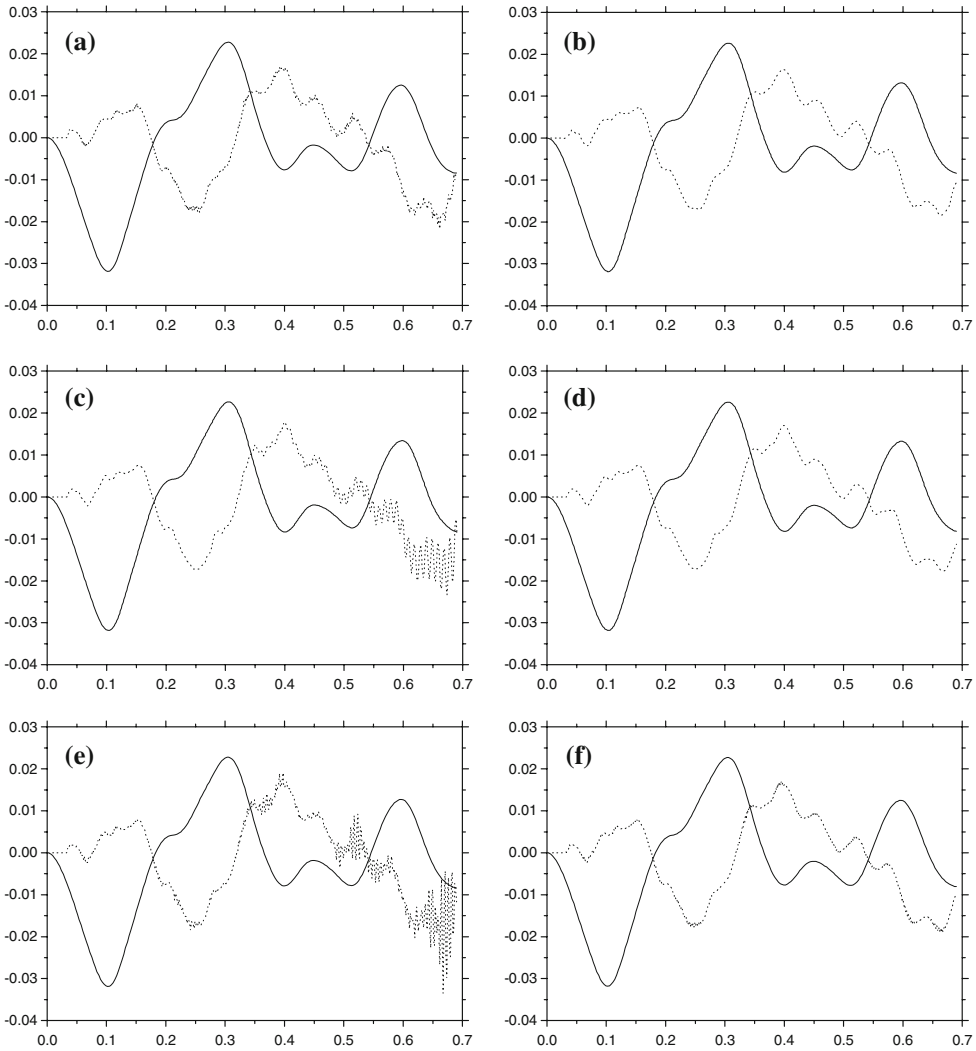

Fig. 8 Scaled vertical displacement (*solid line*) and hydrodynamic pressure (*dot line*) time history results at points A and B, respectively, considering BE stabilization procedures: **a** case 2 ($_s\lambda = 0.00$; $_f\lambda = 0.25$), **b** case 5 ($_s\lambda = 0.25$; $_f\lambda = 0.00$), **c** case 6 ($_s\lambda = 0.25$; $_f\lambda = 0.25$), **d** case 6 ($_s\lambda = 0.75$; $_f\lambda = 0.75$), **e** case 7 ($_s\lambda = 0.00$; $_f\lambda = 0.75$), **f** case 7 ($_s\lambda = 0.25$; $_f\lambda = 0.25$)

Time history results for Case 1 (see Table 1) are depicted in Fig. 5. The results are plotted considering two different water levels, namely $H = 35$ m (seven linear elements with length 5 m are considered to discretize the fluid common interface) and $H = 50$ m (ten linear elements with length 5 m are considered to discretize the fluid common interface). As one can observe, the solution is in good agreement with the results previously presented by von Estorff and Antes [35], considering FEM–BEM coupled analysis.

In Fig. 6, time history results are depicted ($H = 50$ m) considering different interface relations for the coupling of the acoustic and elastodynamic BE formulations. As has been discussed, the present work adopts Eq. (25) to relate $_s\mathbf{U}$ and $_f\mathbf{Q}$. Equation (25) is consistent with the BE formulations in use. Once one takes into account other non-consistent relations to relate $_s\mathbf{U}$ and $_f\mathbf{Q}$ (e.g., Newmark's trapezoidal rule—see Fig. 6, the Houbolt method, etc.), instabilities may occur.

In Fig. 7, time history results considering the different cases of analysis, as described in Table 1, are depicted. As can be seen, for several cases, unstable results arise. In Fig. 8, stabilized BE formulations are considered for the cases where instabilities occur. In Case 6, the adoption of $_s\lambda = 0.25$ and $_f\lambda = 0.25$ is not enough to ensure stability (see Fig. 8c), and more severe stabilization parameters are selected, namely $_s\lambda = 0.75$ and $_f\lambda = 0.75$, ensuring stable results (see Fig. 8d). In Case 7, an analogous situation occurs, as depicted in Figs. 8e,f.

The results presented so far are obtained taking into account a closed-domain dam (null displacements are prescribed at the base of the dam and null fluxes are prescribed at the base of the storage-lake). As is well known, boundary element formulations are an extremely elegant tool to model infinite media. As a consequence, in the present BEM–BEM coupling context, analyses considering an opened-domain dam can be carried out very easily.

In Fig. 4c, the BEM mesh for an opened-domain dam is depicted (the mesh is extended analogously as described in Fig. 4a). For the opened-domain dam analysis, the spatial

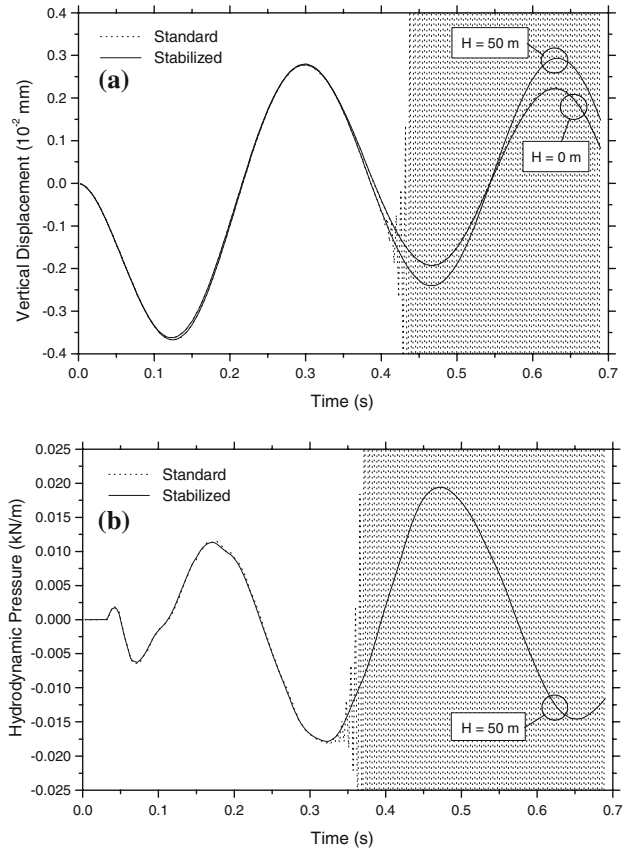

Fig. 9 Time history results for the opened-domain dam–reservoir system considering standard and stabilized (${}_s\lambda = 0.75$; ${}_f\lambda = 0.75$) BE formulations: **a** vertical displacements at point A, **b** hydrodynamic pressures at point B

and temporal discretizations described in Table 1, Case 1, are selected (i.e., there is a perfect connection between the sub-domain nodes on the vertical and horizontal common interfaces).

For the opened-domain dam case, time history results are depicted in Fig. 9, considering two different water levels: $H = 50$ m and $H = 0$ m (no fluid—uncoupled analysis). As one can observe, unstable results arise if standard BE formulations are considered (one should observe that, for the same discretization level, stable results are achieved considering the closed-domain dam); however, stability is ensured once stabilized (${}_s\lambda = 0.75$ and ${}_f\lambda = 0.75$) BE formulations are adopted.

In Fig. 10, some time snap-shots are depicted, describing the displacement evolution of the closed/opened-domain dam.

5.2 Solid wall-confined fluid system

In the previous example, the (dilatational) wave velocities of the different media involved were very similar. These kinds of problems are easier to solve numerically (even so, several numerical instabilities could be observed). In the present example, a more complex (from a numerical standpoint) problem is analyzed [47].

The system under consideration is composed of a rectangular solid wall, coupled to a compressible confined fluid. The model is shown in Fig. 11. At one boundary of the fluid, a distributed horizontal load, acting in time as a rectangular pulse during the first 0.001 s, is prescribed. The material properties of the solid wall are: Poisson's ratio $\nu = 0.29$; Young's modulus $E = 2.068 \times 10^8\,\text{kN/m}^2$; mass density $\rho = 7,820\,\text{kg/m}^3$. The fluid properties are: mass density $\rho = 1,000\,\text{kg/m}^3$; wave velocity $c = 1,000$ m/s (this wave velocity is about six times less than the solid dilatational wave velocity).

As is well known, time-step length plays an important role in the time-domain BEM analyses. A measure of the time-step length is computed according to the following

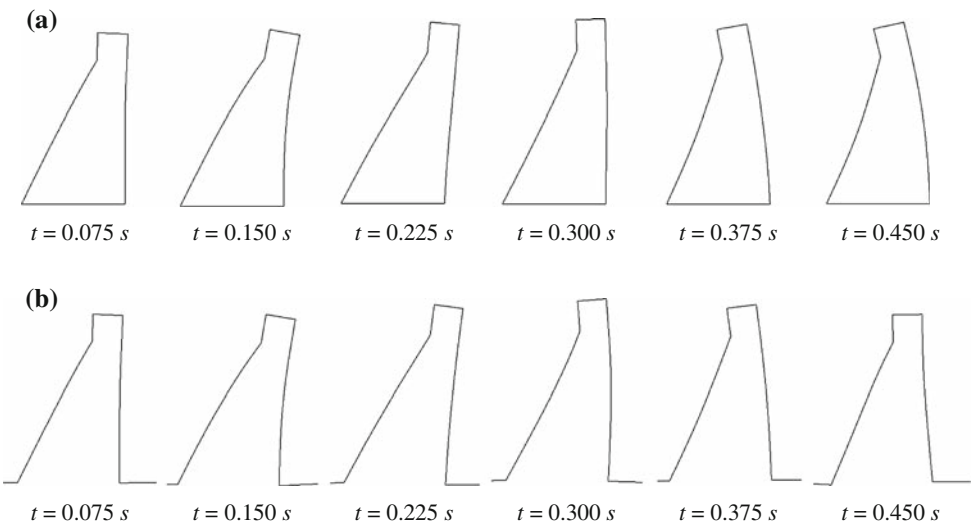

Fig. 10 Scaled displacement results for the dam ($H = 50$ m), along time: **a** closed-domain dam, **b** opened-domain dam

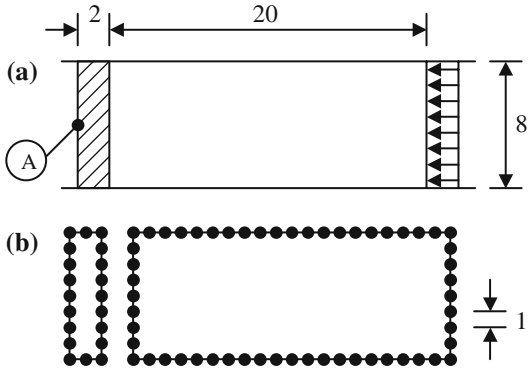

Fig. 11 Sketch of the model: **a** solid wall adjacent to a closed-domain fluid, **b** acoustic and elastodynamic BEM meshes

expression [9]:

$$\beta = c\Delta t/\ell \tag{26}$$

where c is the (dilatational) wave velocity and ℓ is the boundary element length. Practice has shown that for $\beta > 1$ numerical damping is introduced, and that for some smaller β values, instabilities may occur.

In Fig. 12, the transient behaviour of the horizontal displacement at point A is depicted, considering different time-step discretizations (for ${}_f\Delta t = 10^{-3}$ s, ${}_f\beta = 1.00$; for ${}_f\Delta t = 2.5 \times 10^{-4}$ s, ${}_f\beta = 0.25$; for ${}_s\Delta t = 10^{-3}$ s, ${}_s\beta = 5.89$; for ${}_s\Delta t = 2.5 \times 10^{-4}$ s, ${}_s\beta = 1.47$). As one can observe, if standard boundary element formulations are considered, the adoption of different temporal discretizations in each sub-domain is essential, otherwise too damped results may arise (dash line in Fig. 12) or unstable solutions may occur (dot line in Fig. 12). On the other hand, when stabilized boundary element formulations are considered, a wider range of discretization parameters may be adopted, as depicted in Fig. 13, for instance.

As has been highlighted, Eq. (22b) is very effective, concerning stability aspects. Equation (22c) is also extremely effective, but concerning efficiency aspects, as is presented next.

In Fig. 14, time history results are depicted considering the truncation of the BEM time-convolution process. In the present work, the discrete times T_k (see Eq. (23b)), which are the key-times to the interpolation approximation, are evaluated by

$$T_k = T_L + (T_N - T_L)\,((k-1)/(m-1))^{m^{1/2}} \tag{27a}$$

where the time limit T_L is calculated by

$$T_L = \Delta t\, N^{(1-\delta\, m)} + \bar{r}/\bar{c} \tag{27b}$$

In Eq. (27b), δ is a precision control parameter; $\bar{r}$ is the average distance between boundary nodes and $\bar{c}$ is the (average) wave velocity of the medium. The calculus of the time limit T_L is based on the behaviour of function $f(t) = 1/t$, which is a simple function, similar in most aspects to the time related kernels of the models being considered (for more details about expressions (27a,b), the reader is referred to [26]).

Time history results considering different error control parameters (δ) are depicted in Fig. 14 ($m = 10$ is always adopted). As one may observe, accurate results can be obtained for $\delta = 4\%$, $\delta = 5\%$ and $\delta = 6\%$ (for $\delta = 0\%$ complete time-convolution calculations are considered; for $\delta \geq 7\%$ unacceptable miscalculations occur). The reductions achieved on the total CPU time and on the BEM storage area, by

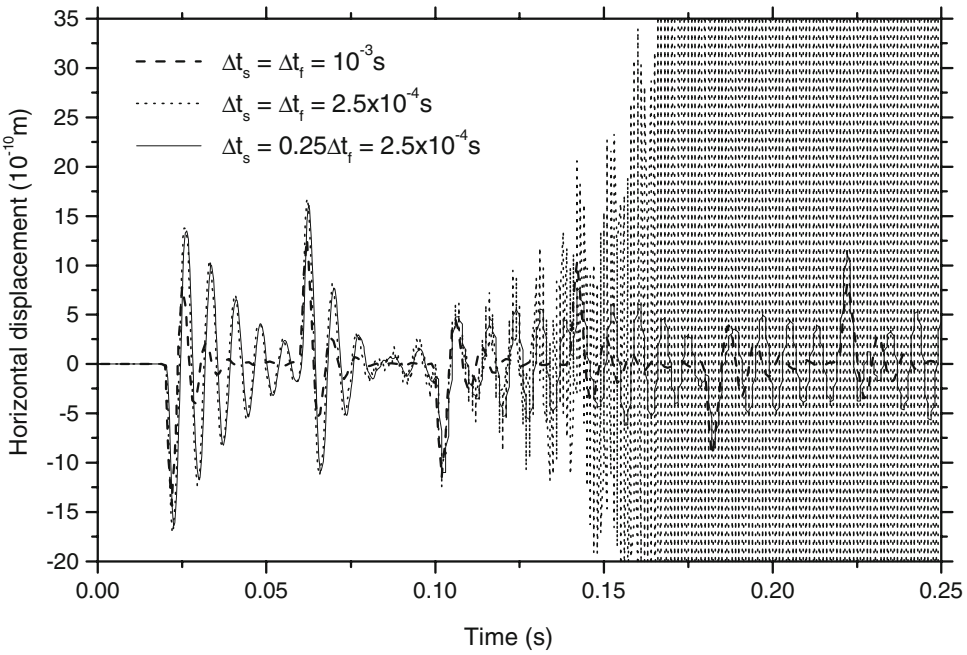

Fig. 12 Horizontal displacement time history results at point A considering different time-steps for the solid and fluid sub-domains

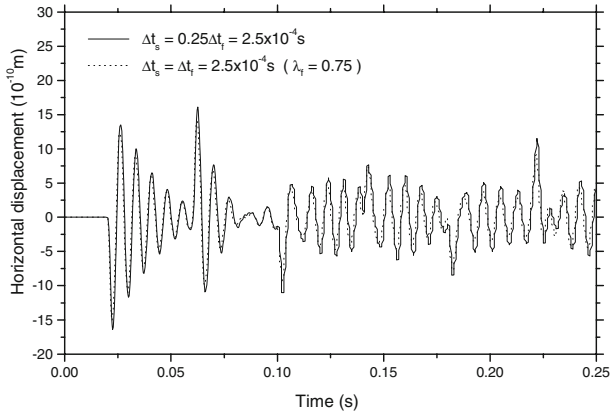

Fig. 13 Horizontal displacement time history results at point A considering standard ($_s\Delta t = 0.25\,_f\Delta t$) and stabilized ($_s\lambda = 0.00; _f\lambda = 0.75$) BE formulations

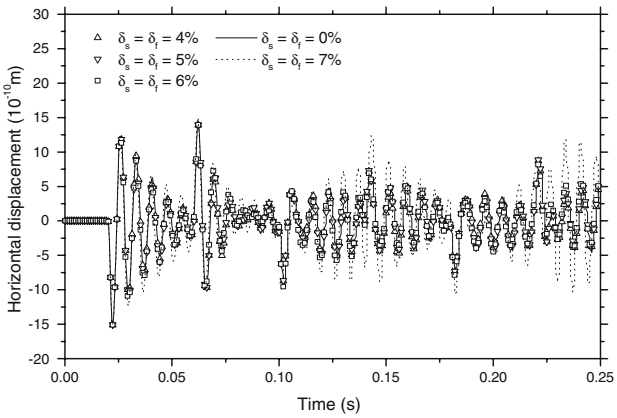

Fig. 14 Horizontal displacement time history results at point A considering a multi-linear interpolation algorithm ($_sm = _fm = 10$) to truncate the BEM time-convolution process ($_s\lambda = 0.00$; $_f\lambda = 0.75$ and $_s\Delta t = _f\Delta t = 2.5 \times 10^{-4}$ s)

Table 2 Cost of the analysis considering truncated time-convolution procedures

δ (%)	Storage area (%)		Total CPU time (%)
	Solid	Fluid	
0	100	100	100
4	6.7	15.6	20
5	4.5	12.5	16
6	2.9	10.9	13
7	2.1	10.1	12

the adoption of the truncated time-convolution procedure, are shown in Table 2. As one can observe, Eq. (22c) drastically reduces time-domain BEM costs, an advantage which is amplified when BEM–BEM coupled analyses are considered.

6 Conclusions

The present work presents an efficient, flexible, accurate and stable algorithm to model the propagation of interacting acoustic–elastic waves using boundary element coupled techniques.

The paper describes several consistent, robust and versatile numerical procedures, namely:

(i) adoption of consistent numerical treatment on common interfaces (improving accuracy and stability);
(ii) adoption of consistent time/space interpolation/extrapolation procedures (improving accuracy, stability, efficiency and flexibility);
(iii) adoption of relaxed iterative coupling procedures (improving stability and efficiency);
(iv) adoption of stabilization parameters into the recent-in-time convolution operations (improving stability);
(v) adoption of time-truncation procedures to compute distant-in-time convolution contributions (improving efficiency).

Two numerical examples are presented at the end of the paper, illustrating the potentialities of the new methodology. In the first example, several combinations of different spatial and temporal discretizations are considered and the developed stabilized algorithm provides proper results for all the cases (one should observe that good results are obtained even considering sub-domain time-step lengths with a difference up to five times, as depicted in Fig. 7h). In the second example, the flexibility, accuracy, stability and efficiency of the proposed algorithm is once again highlighted: good results are obtained at very low computational costs, even though a complex numerical problem is being analysed and standard BE approaches are unable to provide adequate results.

This work extends the applicability and competitiveness of time-domain boundary element techniques, considering the modelling of complex wave propagation phenomena.

References

1. Lombard B, Piraux J (2004) Numerical treatment of two-dimensional interfaces for acoustic and elastic waves. J Comput Phys 195:90–116
2. Collino F, Joly P, Millot F (1997) Fictitious domain method for unsteady problems: application to electromagnetic scattering. J Comput Phys 138:907–938
3. Zhang C, LeVeque RJ (1997) The immersed interface method for acoustic wave equations with discontinuous coefficients. Wave Motion 25:237–263
4. Lombard B (2002) Modélisation Numérique de la Propagation des Ondes Acoustiques et Elastiques en Présence d'Interfaces. Ph.D. Thesis, University of Aix-Marseille II, France
5. Daniel WJT (1997) Analysis and implementation of a new constant acceleration subcycling algorithm. Int J Numer Methods Eng 40:2841–2855

6. Smolinski P (1996) Subcycling integration with non-integer time steps for structural dynamics problems. Comput Struct 59:273–281
7. Belytschko T, Lu YY (1993) Explicit multi-time step integration for first and second order finite element semi-discretization. Comput Methods Appl Mech Eng 108:353–383
8. Soares D Jr, Mansur WJ, Lima DL (2007) An explicit multilevel time-step algorithm to model the propagation of interacting acoustic-elastic waves using finite element/finite difference coupled procedures. Comput Model Eng Sci 17:19–34
9. Mansur WJ (1983) A time-stepping technique to solve wave propagation problems using the boundary element method. Ph.D. Thesis, University of Southampton, England
10. Birgisson B, Siebrits E, Peirce AP (1999) Elastodynamic direct boundary element methods with enhanced numerical stability properties. Int J Numer Methods Eng 46:871–888
11. Frangi A, Novati G (1999) On the numerical stability of time-domain elastodynamic analyses by BEM. Comput Methods Appl Mech Eng 173:403–417
12. Frangi A (2000) Causal shape functions in time domain boundary element method. Comput Mech 25:533–541
13. Carrer JAM, Mansur WJ (2000) Time discontinuous linear traction approximation in time-domain BEM: 2D elastodynamics. Int J Numer Methods Eng 49:833–848
14. Mansur WJ, Carrer JAM, Siqueira EFN (1998) Time discontinuous linear traction approximation in time-domain BEM scalar wave propagation analysis. Int J Numer Methods Eng 42:667–683
15. Yu G, Mansur WJ, Carrer JAM, Gong L (1998) Time weighting in time domain BEM. Eng Anal Bound Elem 22:175–181
16. Araujo FC, Mansur WJ, Nishikava LK (1999) A linear θ time-marching algorithm in 3D BEM formulation for elastodynamics. Eng Anal Bound Elem 23:825–833
17. Yu G, Mansur WJ, Carrer JAM, Gong L (1998) A linear θ method applied to 2D time-domain BEM. Commun Numer Methods Eng 14:1171–1179
18. Yu G, Mansur WJ, Carrer JAM (1999) The linear θ method for 2D elastodynamic BE analysis. Comput Mech 24:82–89
19. Yu G, Mansur WJ, Carrer JAM, Gong L (2000) Stability of Galerkin and collocation time domain boundary element methods as applied to the scalar wave equation. Comput Struct 74:495–506
20. Rizos DC, Karabalis DL (1994) Advanced direct time domain BEM formulation for general 3D elastodynamic problems. Comput Mech 15:249–269
21. Siebrits E, Peirce AP (1997) Implementation and application of elastodynamic boundary element discretization with improved stability properties. Eng Comput 14:669–695
22. Carrer JAM, Mansur WJ (2002) Time-dependent fundamental solution generated by a not impulsive source in the boundary element method analysis of the 2D scalar wave equation. Commun Numer Methods Eng 18:277–285
23. Soares D Jr, Mansur WJ (2007) An efficient stabilized boundary element formulation for 2D time-domain acoustics and elastodynamics. Comput Mech 40:355–365
24. Demirel V, Wang S (1987) An efficient boundary element method for two-dimensional transient wave propagation problems. Appl Math Model 11:411–416
25. Mansur WJ, de Lima Silva W (1992) Efficient time truncation in two-dimensional BEM analysis of transient wave propagation problems. Earthquake Eng Struct Dyn 21:51–63
26. Soares D Jr, Mansur WJ (2004) Compression of time generated matrices in two-dimensional time-domain elastodynamic BEM analysis. Int J Numer Methods Eng 61:1209–1218
27. Carrer JAM, Mansur WJ (2006) Solution of the two-dimensional scalar wave equation by the time-domain boundary element method: lagrange truncation strategy in time integration. Struct Eng Mech 23:263–278
28. Tröndle G, Antes H (2001) Efficient numerical techniques in time and frequency domain, chap. 6. In: von Estorff O (ed) Boundary elements in acoustics, advances & applications, WIT Press, Southampton
29. Tham LG, Chu CK (2000) Some experiences on programming of time domain boundary element in parallel processing environment. J Sound Vib 233:1–17
30. Brebbia CA (1978) The boundary element method for engineers. Pentech Press, London
31. Zienkiewicz OC, Kelly DM, Bettess P (1977) The coupling of the finite element method and boundary solution procedures. Int J Numer Methods Eng 11:355–376
32. Brebbia CA, Georgiou P (1979) Combination of boundary and finite elements in elastostatics. Appl Math Model 3:212–220
33. Karabalis DL, Beskos DE (1985) Dynamic response of 3D flexible foundations by time domain BEM and FEM. Solid Dyn Earthquake Eng 4:91–101
34. von Estorff O, Prabucki MJ (1990) Dynamic response in time domain by coupled boundary and finite elements. Comput Mech 6:35–46
35. von Estorff O, Antes H (1991) On FEM–BEM coupling for fluid–structure interaction analysis in the time domain. Int J Numer Methods Eng 31:1151–1168
36. von Estorff O (1992) Coupling of BEM and FEM in the time domain: some remarks on its applicability and efficiency. Comput Struct 44:325–337
37. Belytschko T, Lu YY (1994) A variational coupled FE-BE method for transient problems. Int J Numer Methods Eng 37:91–105
38. von Estorff O, Firuziaan M (2000) Coupled BEM/FEM approach for nonlinear soil/structure interaction. Eng Anal Bound Elem 24:715–725
39. Czygan O, von Estorff O (2002) Fluid–structure interaction by coupling BEM and nonlinear FEM. Eng Anal Bound Elem 26:773–779
40. Yu G, Mansur WJ, Carrer JAM, Lie ST (2001) A more stable scheme for BEM/FEM coupling applied to two-dimensional elastodynamics. Comput Struct 79:811–823
41. Yu GY, Lie ST, Fan SC (2002) Stable boundary element method/finite element method procedure for dynamic fluid structure interactions. J Eng Mech 128:909–915
42. Soares D Jr (2004) Dynamic analysis of non-linear soil–fluid-structure coupled systems by the finite element method and the boundary element method (in Portuguese). Ph.D. Thesis, Federal University of Rio de Janeiro, Brazil
43. Elleithy WM, Al-Gahtani HJ (2000) An overlapping domain decomposition approach for coupling the finite and boundary element methods. Eng Anal Bound Elem 24:391–398
44. Elleithy WM, Al-Gahtani HJ, El-Gebeily M (2001) Iterative coupling of BE and FE methods in elastostatics. Eng Anal Bound Elem 25:685–695
45. Soares D Jr , von Estorff O (2004) Combination of FEM and BEM by an iterative coupling procedure. In: 4th European congress on computational methods in applied sciences and engineering, ECCOMAS 2004, Jyväskylä, Finland
46. Soares D Jr, von Estorff O, Mansur WJ (2004) Iterative coupling of BEM and FEM for nonlinear dynamic analyses. Comput Mech 34:67–73
47. Soares D Jr, von Estorff O, Mansur WJ (2005) Efficient nonlinear solid–fluid interaction analysis by an iterative BEM/FEM coupling. Int J Numer Methods Eng 64:1416–1431
48. von Estorff O, Hagen C (2005) Iterative coupling of FEM and BEM in 3D transient elastodynamic. Eng Anal Bound Elem 29:775–787
49. Carrer JAM, Telles JCF (1992) A boundary element formulation to solve transient dynamic elastoplastic problems. Comput Struct 13:707–713

50. Soares D Jr, Carrer JAM, Mansur WJ (2005) Non-linear elastodynamic analysis by the BEM: an approach based on the iterative coupling of the D-BEM and TD-BEM formulations. Eng Anal Bound Elem 29:761–774
51. Soares D Jr, Mansur WJ (2006) Dynamic analysis of fluid–solid–structure interaction problems by the boundary element method. J Comput Phys 219:498–512
52. Soares D Jr, Mansur WJ (2007) Iterative coupling of different boundary element formulations: applications concerning time-domain nonlinear analysis of fluid-soil-structure coupled systems. In: XXVIII Iberian Latin American congress on computational methods in engineering, CILAMCE 2007, Porto, Portugal
53. Hadamard J (1952) Lectures on Cauchy's problem in linear partial differential equations. Dover Publications, New York
54. Dominguez J (1992) Boundary elements in dynamics. Computational Mechanics Publications, Southampton
55. Carrer JAM, Mansur WJ (1993) Two-dimensional transient BEM analysis for the scalar wave equation: kernels. Eng Anal Bound Elem 12:283–288
56. Soares D Jr, Carrer JAM, Telles JCF, Mansur WJ (2002) Numerical computation of internal stress and velocity in time-domain BEM formulation for elastodynamics. Comput Mech 30:38–47
57. Newmark NM (1959) A method of computation for structural dynamics. ASCE J Eng Mech Div 85:67–94
58. Czygan O (2002) Fluid/Struktur-Kopplung bei ebenen und rotationssymmetrischen Systemen unter Berücksichtigung nichtlinearen Strukturverhaltens. Ph.D. Thesis, TU Hamburg-Harburg, Germany